

Influence of Na₂O Content on Lattice Structures of Iron Oxides during Reduction Process of Fe₂O₃ Briquetting

Guo-Ping LUO^{1,a,*}, Quan SUN^{1,b}, Yong-Bin WANG^{1,2,c} and Jian-Guo ZHU^{1,d}

¹Material and Metallurgy School, Inner Mongolia University of Science and Technology, Baotou 014010, Nei Mongol, China

²School of Metallurgical and Ecological Engineering, University of Science and Technology, Beijing 100083, Beijing, China

^aluoguoping3@126.com, ^bbtsunquan@126.com, ^cbtwangyongbin@126.com, ^dzhujianguo@163.com, *Corresponding author

Key words: Na₂O, Iron oxides, Reduction, Lattice structure, Liquid phase, Solid solution

Abstract: In order to fill up the deficiency of the theoretical basis about reduction swelling during Bayan Obo iron concentrate roasting and reduction process, The influence of Na₂O content on lattice structures of iron oxides at different reduction stages of Fe₂O₃ briquetting has been investigated by using the method of ‘briquetting-roasting-reduction’ and the raw material is ferric oxide(Fe₂O₃), anhydrous sodium carbonate(Na₂CO₃) provided by Shanghai Chemical Reagent Company of Chinese Medical Group, The result shows that at roasting stage of Fe₂O₃ briquetting, Na₂O content has no obvious effect on Fe₂O₃ lattice structure, and Na₂CO₃ tends to react with Fe₂O₃, which produces some low melting point ferrate like NaFeO₂ and liquid phase; at reduction stage from Fe₂O₃ to Fe₃O₄, Fe₃O₄ has a stable crystal structure and its lattice parameter significantly increases due to the solid solution and liquid phase formed in reduction and roasting processes, respectively, at reduction stage from Fe₂O₃ to Fe_xO, the XRD diffraction peak of Fe_xO shifts towards the small angle with the increase of Na₂O content, resulted from the formation of solid solution; at reduction stage from Fe₂O₃ to Fe, Na₂O has no obvious effect on the lattice parameter and the crystal cell volume of Fe because of its gasification and volatilization at the reduction temperature of 1000 °C.

Introduction

Owing to the high alkali metal content in Baiyunebo iron concentrates [1, 2], the pellets containing alkali metals are detrimental to the blast furnace condition in the iron-making process [3,4]. On the one hand, the volume expansion of pellets is serious during reduction process, which has bad influence on the burden descending [5-7], on the other hand, the gangue has the lower softening point, which accelerates the formation of furnace slag and decreases the blast furnace permeability [8-10]. Therefore, the effect of alkali metal on reduction process of iron oxides has attracted increasing attention. Moreover its mechanism is not clear so far, especially the influence of alkali metal on the crystal structure of iron oxide in different stages of reduction, which affect the whole process [11-14]. The lattice constant is an important parameter in the crystal structure, and its variability reflects the changes of the interior crystal compositions and stress state. And this article can provide useful information to explore pellets reduction expansion mechanism and understand iron oxide reduction mechanism. The paper to investigate the influence of alkali metals on lattice structures of iron oxides at different reduction stages, will play an important role in revealing the mechanism of abnormal reduction expansion of pellets produced by Baiyunebo iron concentrates.

1 Experimental Materials and Methods

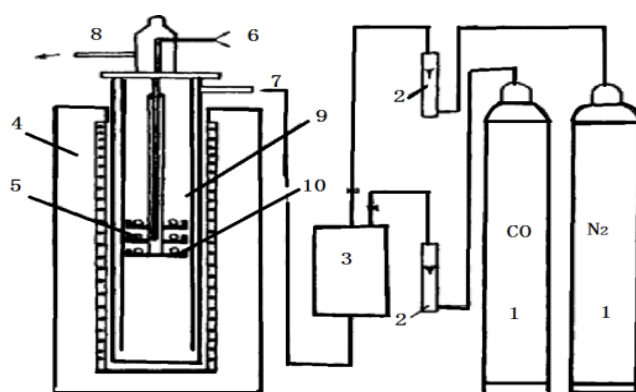
1.1 Raw Materials and Preparation

Ball milling mixing tank was adopted to mix raw materials prepared in advance. The mixing time remains more than 5h for a good mixing. The mixed materials were firstly dried in the blast oven at

80°C, and then compressed into a diameter of 20mm, round pie clumps 4g weight by the DY-20 electric hydraulic system prototype while the pressure was 8MPa and die-casting time was 2min. Then, the clump sample was placed in the box-type resistance furnace at 1280°C, solid phase calcined for 2h in an air atmosphere. Finally, the clump sample was cooled to room temperature with the furnace and set aside. The briquetting samples were prepared by using the pure reagent Fe_2O_3 as basic material and Na_2CO_3 instead of Na_2O . The contents of Na_2O were 0wt%, 1wt% and 5wt%, respectively, in samples 1#, 2# and 3#.

1.2 Experimental Methods

According to the principles of fractional reduction of iron oxides, the Fe_2O_3 briquetting was reduced into Fe through three stages, namely, $\text{Fe}_2\text{O}_3 \rightarrow \text{Fe}_3\text{O}_4$, $\text{Fe}_2\text{O}_3 \rightarrow \text{Fe}_x\text{O}$ and $\text{Fe}_2\text{O}_3 \rightarrow \text{Fe}$. The reduction equipment is shown in the following figure 1.



1-gas bottle; 2-flowmeter; 3-mixer; 4-reduction furnace; 5-samples; 6-thermocouple; 7-gas inlet; 8-gas outlet; 9- reduction tube; 10-experimental container

Fig.1 The schematic diagram of reduction equipment

Based on equilibrium diagram of CO reducing iron oxides and the thermal dynamic software FactSage 6.2, the temperature, time and atmosphere in the whole reduction process were determined to ensure that the pure Fe_2O_3 could be completely reduced into iron oxides of the next step. The experimental parameters of each reduction stage were listed in table 1.

Table 1 Experimental parameters of each reduction stage

Reduction stage	Temperature/(°C)	CO/(L·h ⁻¹)	N ₂ /(L·h ⁻¹)	Gas flow/(L·h ⁻¹)	Time/(h)
$\text{Fe}_2\text{O}_3 \rightarrow \text{Fe}_3\text{O}_4$	650	150	450	600	1
$\text{Fe}_2\text{O}_3 \rightarrow \text{Fe}_x\text{O}$	900	420	180	600	1
$\text{Fe}_2\text{O}_3 \rightarrow \text{Fe}$	1000	600	--	600	1

The roasted and reduced products were analyzed by X-ray diffraction (XRD, D8X) and lattice parameters of Fe_xO and Fe were calculated by means of X-ray diffraction patterns. Besides, the effect of Na_2O content on the crystal structure reduction swelling of iron oxides was further revealed by applying differential thermal analysis (DTA).

2 Results and Discussion

2.1 Influence of Na_2O on the Lattice Structure of Fe_2O_3

The 1#, 2# and 3# samples were roasted according to the designed process and then characterized by XRD respectively, as shown in Fig. 2.

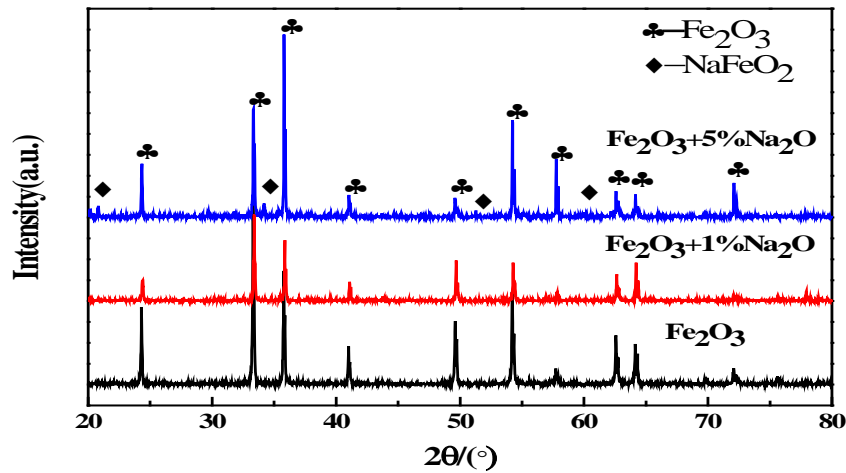


Fig.2 X-ray diffraction patterns of roasted Fe_2O_3 briquetting samples

Fig. 2 shows that, some NaFeO_2 was formed in the briquetting sample with 5% Na_2O during roasting process. By means of the thermodynamic software (Factsage 6.2) calculation, the reaction was as follows.



The product NaFeO_2 has a low melting point. A liquid phase can be clearly observed in the roasted samples added with the Na_2O , which resulted in the deformation of the samples. The sample is shown in the following figure3.



Fig.3 The briquetting samples after roasted

To confirm this reaction, the solid phase reactions of Fe_2O_3 - Na_2CO_3 system were investigated using differential thermal analysis. As shown in Fig. 4, there appear two endothermic peaks at 132.9 °C and 839.6 °C on DTA curve, and each peak is accompanied by weightlessness, which indicates that the solid phase reactions with gas evolving happened. Because of a strong endothermic reaction the endothermic peak area corresponding to 839.6 °C is becoming larger.

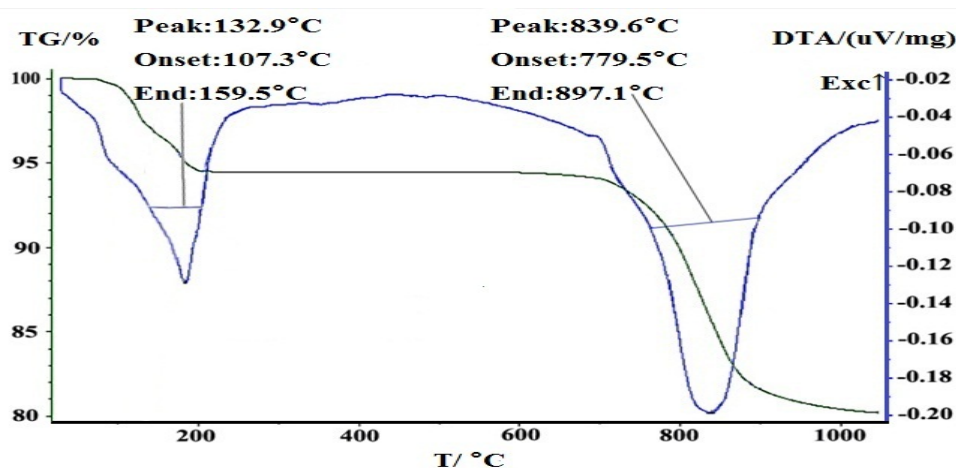


Fig.4 DTA - TG curve of Fe_2O_3 - Na_2CO_3 solid phase reaction system

The results of studies on the solid phase reactions of Na_2O - CaO - Fe_2O_3 system reported by Qi^[15] indicated that a clear endothermic peak at 820 °C could be attributed to the formation of NaFeO_2 . Hence, the endothermic peak at 839.6 °C is considered to be ascribed to the formation reaction of NaFeO_2 and the decomposition reaction of Na_2CO_3 whose generating temperature is in the range from 779.5°C to 839.6 °C. Because the melting point of Na_2CO_3 is 851 °C and its decomposition reaction occurs after melting, it can be deduced from related literatures that the endothermic peak at 132.9 °C corresponds to free water evaporation.

To explore the influence of Na_2O on the lattice structures of iron oxides, the lattice parameter, axial ratios, and cell volumes of 1#, 2# and 3# samples were calculated respectively, by means of XRD patterns and related formulas of lattice geometry [16], as listed in Table 2.

Table 2 Lattice parameters of Fe_2O_3 in briquetting samples after roasted

Samples	Lattice parameter (a=b, c/ Å)		Axial ratio c/a	Unit-cell volume (Å ³)
1#	5.0242	13.7072	2.7282	299.6493
2#	5.0271	13.7017	2.7256	299.8749
3#	5.0259	13.7046	2.7267	299.7952

As shown in Table 2, compared with 1# sample without adding Na_2O , the lattice constants of iron oxides of 2# and 3# samples containing Na_2O have changed little during the same roasting process. It is considered that Na_2O has no influence on the lattice structure of Fe_2O_3 at roasting stage, because the variations of the lattice constants are generally in a magnitude of 10^{-1} - 10^{-2} Å.

2.2 Influence of Na_2O on the Lattice Structure of Fe_3O_4 at Reduction Stage from Fe_2O_3 to Fe_3O_4

After roasting, the Fe_2O_3 briquetting samples were reduced to Fe_3O_4 according to the designed process in Table 1 and the reduction products were subjected to XRD detections, as shown in Fig. 5.

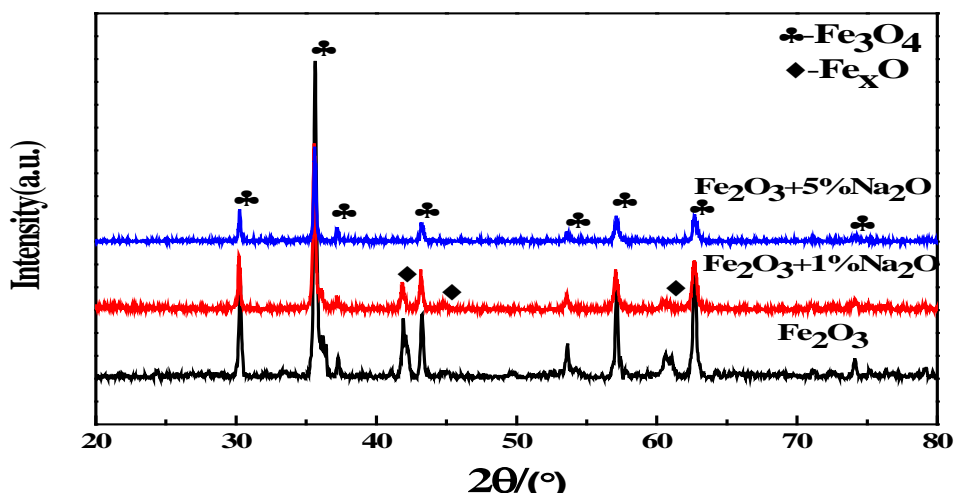


Fig.5 X-ray diffraction patterns of the products at reduction stage of $\text{Fe}_2\text{O}_3 \rightarrow \text{Fe}_3\text{O}_4$

Under the same reduction process, the reduction products are mainly Fe_3O_4 and a spot of Fe_xO for 1# and 2# samples with Na_2O contents of 0% and 1% respectively, but for 3# sample with Na_2O content of 5%, the reduction products are almost entirely the target product Fe_3O_4 . The reason is mainly the formation of some liquid phase in the briquetting samples containing Na_2O during the roasting process, which fills the pores of the samples, and furthermore, hinders the diffusion of reducing gas and the reduction of Fe_3O_4 to the low-valence iron oxide Fe_xO . The higher Na_2O content in the samples, the more liquid phase appears during the roasting process and the greater hindering effect on the reduction of Fe_3O_4 is, which is verified by XRD patterns. A similar result was reported by related study [17]. The less Na_2O additive in the samples, the higher reduction degree of iron oxide. Although the lattice structures of Fe_3O_4 and Fe_xO are not completely consistent, they both belong to the cubic structure and exhibit the better corresponding degree of lattice orientation. Therefore, the deformation energy required for the lattice transformation from Fe_3O_4 to Fe_xO is relatively small, and it is easier to reduce Fe_3O_4 to Fe_xO . Although some NaFeO_2 appeared in 3# roasted sample, the diffraction peak of NaFeO_2 wasn't detected in 3# reduced sample by XRD. This is due to the better thermodynamic and kinetic conditions of NaFeO_2 reduction, under which NaFeO_2 was reduced to Fe_3O_4 and Na^+ ions were solid dissolved in Fe_3O_4 crystal lattice. The solid solution of Na^+ ions increases the stability of the lattice structure of Fe_3O_4 , and has a positive impact on the reduction from Fe_2O_3 to Fe_3O_4 and a negative impact on the reduction from Fe_3O_4 to Fe_xO , hence the reduction products of 3# sample are almost Fe_3O_4 . To further confirm the above phenomenon, the lattice parameters of the reduction product Fe_3O_4 in different samples were calculated, as demonstrated in Table 3.

Table 3 Lattice parameters of the product Fe_3O_4 at reduction stage of $\text{Fe}_2\text{O}_3 \rightarrow \text{Fe}_3\text{O}_4$

Samples	Lattice parameter($a=b=c/\text{Å}$)	Unit-cell volume (Å^3)
1#	8.3496	582.0992
2#	8.3668	585.7040
3#	8.3727	586.9439

It was found that the lattice constants of the product Fe_3O_4 in 2# and 3# samples with Na_2O additive are larger than that of 1# sample without Na_2O under the same reduction process and it increases when the Na_2O content increases from 1% to 5%. The reasons are as follows: metals Na and Fe both belong to body-centered cubic structure; supposing that r_1 and r_2 are defined as the radii of Na^+ ion and Fe^{3+} ion, a continuous solid solution can be formed only when the two kinds of ionic structures are same as well as $(r_1 - r_2) / r_2 < 15\%$; when $(r_1 - r_2) / r_2 = 15\% - 30\%$ a limited solid solution can be formed; when $(r_1 - r_2) / r_2 > 30\%$ it is fairly difficult to form a solid solution but easy

to form the intermediate phase or compound [18]. Therefore, it is very hard for Na^+ and Fe^{3+} to form a solid solution but easy to form sodium ferrite during the roasting process. The radii of Na^+ ion, Fe^{2+} ion and Fe^{3+} ion are 0.095 nm, 0.076 nm and 0.064 nm respectively [19-21], and the relationship between the radii of Na^+ ion and Fe^{2+} ion is $(r_1 - r_2) / r_2 = 25\%$, Which is in the range of 15%-30%, namely, Na^+ ion can substitute Fe^{2+} ion to form a limited solid solution. Therefore, during the reduction process from Fe_2O_3 to Fe_3O_4 , a part of Na^+ ion solid dissolved in the Fe_3O_4 crystal lattice for the briquetting samples with Na_2O additive. Because Fe^{2+} ion and Na^+ ion are not equivalent, they can only form a limited substitutional solid solution [22]. In addition, the solid solution of Na^+ ion with the larger radius than Fe^{2+} ion leads to the rise of lattice constant and cell volume of Fe_3O_4 , and eventually increases the reduction swelling rate. As the formation of solid solution tends to prevent the phase transformation of crystal, the solid solution plays an important role in stabilizing the lattice structure.

2.3 Influence of Na_2O on the lattice structure of Fe_xO at reduction stage from Fe_2O_3 to Fe_xO

After roasting, the Fe_2O_3 briquetting samples were reduced to Fe_xO according to the designed process in Table.1 and the reduction products were subjected to XRD detections, as shown in Fig. 6.

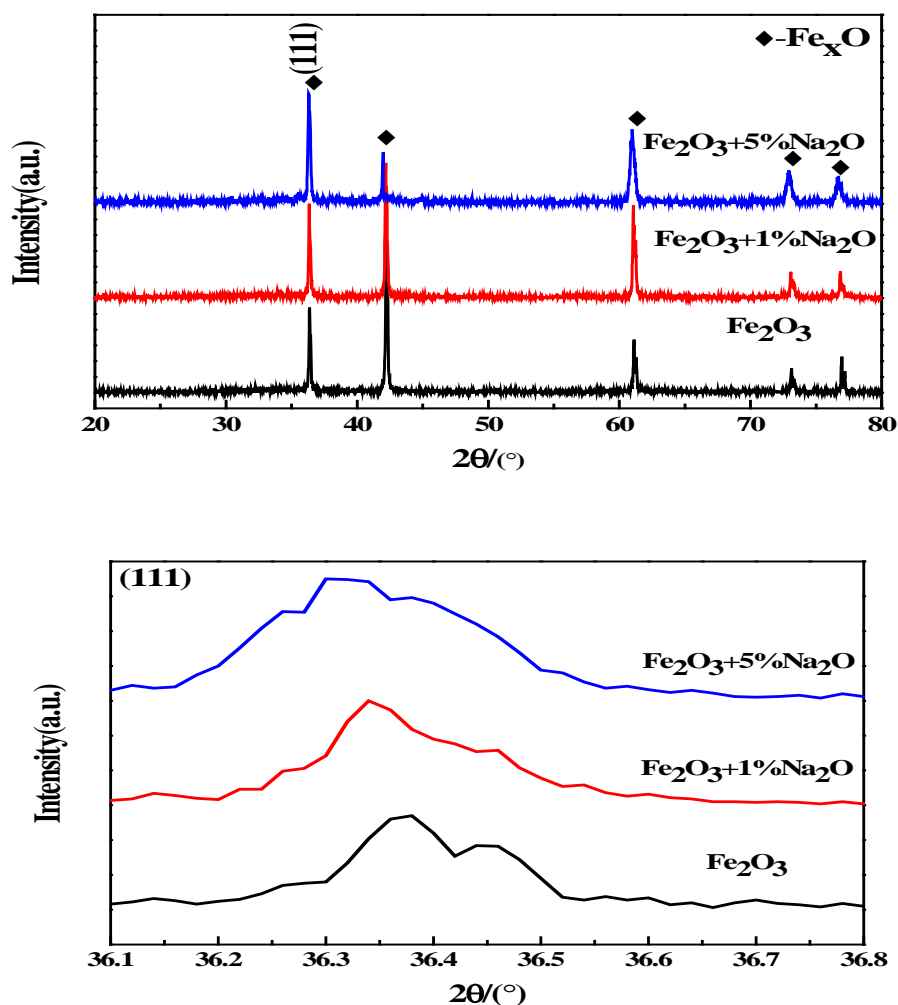


Fig.6 X-ray diffraction patterns of the products at reduction stage of $\text{Fe}_2\text{O}_3 \rightarrow \text{Fe}_x\text{O}$

XRD results show that all samples with different addition levels of Na_2O were reduced to the target product Fe_xO under the same reduction condition. Because NaFeO_2 generated at the roasting stage was also reduced to Fe_xO , its diffraction peaks have not been detected. With NaFeO_2 being reduced, Na^+ ions solid-dissolved into the crystal lattice of Fe_xO , hence no sodium compounds were

detected by XRD. XRD results indicate that the diffraction peak position of Fe_xO shifts towards the small angle range with the increasing Na_2O content, which is due to the solid solution of Na^+ ions in Fe_xO . The enlarged diffraction peak of crystal plane (111) was given in Fig.6. It has been shown from the Bragg equation $2d\sin\theta=n\lambda$ that the shift of diffraction peak position towards small-angle range indicates the interplanar distance becoming larger. Because Fe_xO belongs to cubic system, the interplanar distance is proportional to the lattice constant. Therefore, the shift of diffraction peak position towards small-angle range shows the lattice constant and reduction swelling rate increasing eventually. The lattice parameters of the reduction product Fe_xO were calculated for the briquetting samples with different contents of Na_2O , shown in the table 4.

Table 4 Lattice parameters of the product Fe_xO at reduction stage of $\text{Fe}_2\text{O}_3 \rightarrow \text{Fe}_x\text{O}$

Samples	Lattice parameter (a=b=c/ Å)	Unit-cell volume (Å^3)
1#	4.2833	78.5842
2#	4.2872	78.7991
3#	4.2934	79.1415

From the observed facts it is known that the lattice constant and cell volume of the target product Fe_xO increase with the addition amount of Na_2O increasing. Because the radius of Na^+ ion is larger than Fe^{2+} ion, the substitution of Fe^{2+} ions with Na^+ ions leads to the atomic lattice of Fe_xO swelling and the lattice constant as well as cell volume increasing.

2.4 Influence of Na_2O on the Lattice Structure of Fe at Reduction Stage from Fe_2O_3 to Fe

According to the designed process in Table 1 the Fe_2O_3 briquetting samples roasted were reduced to Fe and the X-ray diffraction analysis of the reduction products is shown as Figure 7.

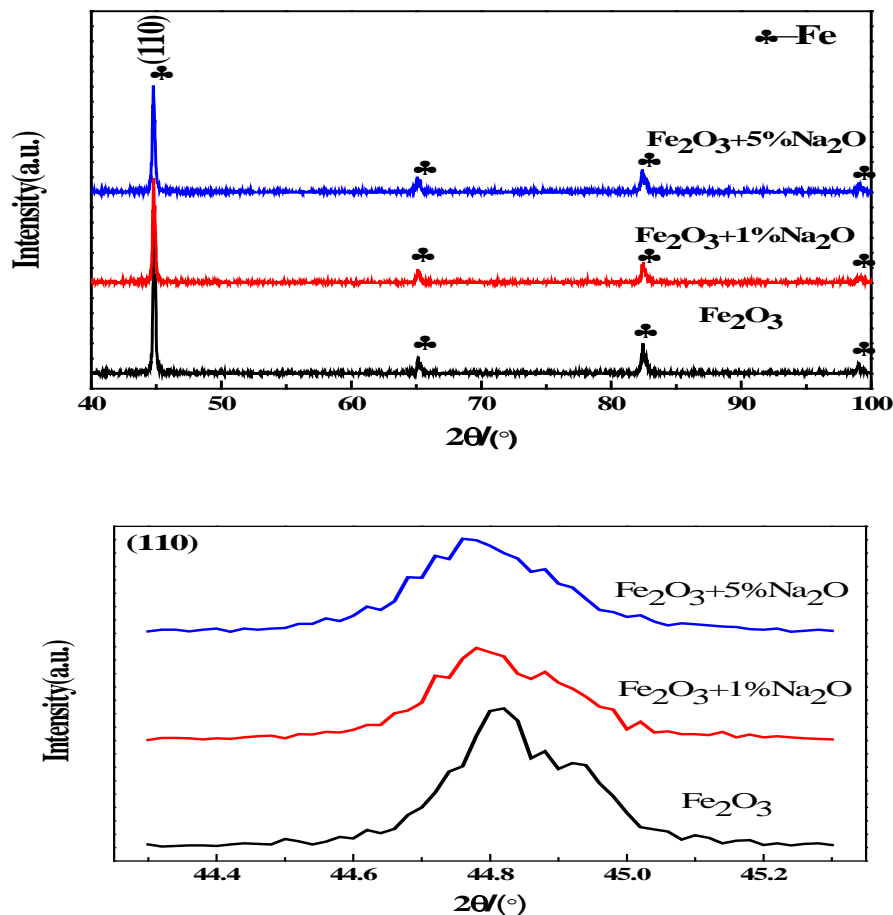


Fig.7 X-ray diffraction patterns of the products at reduction stage of $\text{Fe}_2\text{O}_3 \rightarrow \text{Fe}$

By analysis, we can know that three samples with different addition amount of Na_2O were reduced to the target product Fe under the same reduction process, while no sodium compounds were detected. This is because Na^+ ions and O^{2-} ions in Fe_xO combined to form Na_2O with Fe_xO being reduced to Fe. The melting point and boiling point of Na_2O are $611.1\text{ }^\circ\text{C}$ and $690.6\text{ }^\circ\text{C}$ respectively, so Na_2O is easily to gasify and difficult to exist in the reduction product Fe at the reduction temperature of $1000\text{ }^\circ\text{C}$. For each sample the diffraction peak position of the reduction product Fe does not shift obviously. That is to say, Na_2O would not impact on crystalline form of reduction product. The results of lattice parameters of the product metallic iron for each sample are shown as Table 5.

Table 5 Lattice parameters of the product Fe at reduction stage of $\text{Fe}_2\text{O}_3 \rightarrow \text{Fe}$

Samples	Lattice parameter ($a=b=c/\text{Å}$)	Unit-cell volume (Å^3)
1#	2.8597	23.3865
2#	2.8604	23.4035
3#	2.8612	23.4231

By the data analysis in Table 5, the lattice parameters of the reduction products for three samples with different content of Na_2O are highly similar. Because of the gasification and volatilization of Na_2O at the higher reduction temperature, the lattice structure of the product metal iron was not affected by the content of Na_2O .

Conclusions

1. At roasting stage of Fe_2O_3 briquetting, Na_2O has no obvious effect on the lattice structure of Fe_2O_3 , but Na_2CO_3 easily reacts with Fe_2O_3 to generate low melting point NaFeO_2 , and the starting temperature of the solid phase reaction is $779.5\text{ }^\circ\text{C}$. Moreover, the melting point of Na_2CO_3 is only $851\text{ }^\circ\text{C}$ and its decomposition reaction occurs after melting, so some liquid phase would generate at this stage.

2. At reduction stage from Fe_2O_3 to Fe_3O_4 , Na_2O has obvious effect on the lattice parameters of the product Fe_3O_4 . Na^+ ions can solid dissolve in Fe_3O_4 lattice, which leads to the lattice constant and cell volume of Fe_3O_4 increasing and the reduction swelling rate increasing eventually.

3. At reduction stage from Fe_2O_3 to Fe_xO , the diffraction peak of Fe_xO shifts towards the small-angle range with the increase of Na_2O content, which increases the lattice parameter and cell volume of Fe_xO . Because Na^+ ions with larger radius dissolve in Fe_xO lattice, which promotes the formation of the limited substitutional solid solution.

4. At reduction stage from Fe_2O_3 to Fe, Na_2O has no effect on the lattice structure of the product metal iron because of the gasification and volatilization of Na_2O at the reduction temperature of $1000\text{ }^\circ\text{C}$.

Acknowledgments

This work was financially supported by National Natural Science Foundation of China (Grant 51364030).

References

- [1] G. P. Luo, S. L. Wu, Y. C. Wang, G. J. Zhang, Z. Z. Zhong, H. L. Wu. *Adv. Mater. Res.* 194-196 (2011) 201-206.
- [2] G. P. Luo, S. L. Wu, G. J. Zhang, Y. C. Wang. *J. Iron Steel Res. Int.* 20 (2013) 18-23.
- [3] N. B. Ballal. *Trans. Indian Inst. Met.* 66 (2013) 483-489.
- [4] Alexander V. Zabula; Brian S. Dolinar, Robert West. *J. Organomet. Chem.* 751 (2014) 258-461.

- [5] P. F. Nogueira, R. J. Fruehan. *Metall. Mater. Trans. B* 36 (2004) 829-838.
- [6] P. F. Nogueira, R. J. Fruehan. *Metall. Mater. Trans. B* 36 (2005) 583-590.
- [7] P. F. Nogueira, R. J. Fruehan. *Metall. Mater. Trans. B* 37 (2006) 551-558.
- [8] N. Takeuchi, Y. Lwami, T. Higuchi, K. Nushiro, N. Oyama, M. Sato. *ISIJ Int.* 54 (2014) 791-800.
- [9] K. Yamaguchi, K. Higuchi, Y. Hosotani, S. A. Kasama. *Trans. Iron Steel Inst. Jpn.* 84 (1998) 702-708.
- [10] X. H. Fan, M. Gan, T. Jiang, L. S. Yuan, X. L. J. *Cent. South Univ. Technol.* 17 (2010) 732-737.
- [11] S. Dwarapudi, T. K. Ghosh, A. Shankar, V. Tathavadkar, D. Bhattacharjee, R. Venugopal. *Int. J. Miner. Process.* 96 (2010) 45-53.
- [12] M. Jallouli, F. Ajersch. *J. Mater. Sci.* 21 (1986) 3528-3538.
- [13] S. Dwarapudi, T. K. Ghosh, V. Tathavadkar, M. B. Denys, D. Bhattacharjee, R. Venugopal. *Int. J. Miner. Process.* 112 (2012) 55-62.
- [14] P. Alizadeh, M. Yousefi, B. Eftekhari, N. Ghafoorian, F. Molaie *Ceram. Int.* 33 (2007) 767-771.
- [15] L. K. Qi. *Yu Se Chin Shu, Yeh Lien Pu Fen*, 10 (1965) 50-53. (in Chinese)
- [16] S. M. Allen, E. L. Thomas. *The Structure of Materials*. New York: Wuley, 1998.
- [17] W. Pan, K. Wu, Y. Zhao, Z. X. Zhao, D. J. Min. *Kang T'ieh*, 48 (2013) 7-14. (in Chinese)
- [18] Richard J.D. Tilley. *Defects in Solids*. Peking University Press. BeiJing: China, 2013.
- [19] R. M. Cornell, U. Schwertmann. *VCH Publishers*. New York: US, 1996.
- [20] G. T. Burstein, *Corros. Sci.* 39 (1997) 1499-1500.
- [21] P. Poth, *Mater. Corros.* 55 (2004) 704.
- [22] X. L. Song, X. H. Huang. *Chemical industry press*. Beijing: China, 2005.